# Metallo-Supramolecular Structures by Self-Assembly through Weak Interactions in Mixed Ligand Metal Complexes of Adenine and Malonate

**ARTICLE** *in* CRYSTAL GROWTH & DESIGN · DECEMBER 2013

Impact Factor: 4.89 · DOI: 10.1021/cg401455c



**5 AUTHORS**, INCLUDING:

Alfonso Castineiras
University of Santiago de Compostela
**446** PUBLICATIONS **7,253** CITATIONS
SEE PROFILE

Isabel García-Santos
University of Santiago de Compostela
**42** PUBLICATIONS **790** CITATIONS
SEE PROFILE

Josefa María González-Pérez
University of Granada
**78** PUBLICATIONS **833** CITATIONS
SEE PROFILE

CRYSTAL GROWTH & DESIGN

Article

pubs.acs.org/crystal

# Metallo-Supramolecular Structures by Self-Assembly through Weak Interactions in Mixed Ligand Metal Complexes of Adenine and Malonate

H. El Bakkali,[‡] A. Castiñeiras,*[,†] I. García-Santos,[†] J. M. González-Pérez,[‡] and J. Niclós-Gutiérrez[‡]

[†]Department of Inorganic Chemistry, Faculty of Pharmacy, University of Santiago de Compostela, E-15782 Santiago de Compostela, Spain

[‡]Department of Inorganic Chemistry, Faculty of Pharmacy, University of Granada, E-18071 Granada, Spain

Supporting Information

**ABSTRACT:** The reactions of sodium malonate with $Co^{II}$, $Cu^{II}$, or $Zn^{II}$ salts in the presence of adenine afforded the compounds $[Co(7H\text{-ade-}N9)_2(H_2O)_4][Co(\kappa^2\text{-mal})(H_2O)_2]\cdot 4H_2O$ (**1**), $_\infty{}^1[Cu(\mu\text{-mal})(7H\text{-ade-}N9)(\mu_2\text{-}H_2O)]$ (**2**), and $[Zn_2(\mu\text{-mal})_2(\mu\text{-}7H\text{-ade-}N3,N9)_2(H_2O)_2]\cdot 2H_2O$ (**3**), all of which have been characterized by elemental analyses, mass spectrometry, FT-IR, electronic and EPR spectroscopy, magnetic measurements, and single-crystal X-ray diffraction. Complex **1** is an ion-pair product managed by charge-assisted noncovalent interactions. Complex **2** is formed by binuclear $[Cu(mal)(Hade)(H_2O)]_2$ units bridged by malonate ligands, and 1D coordination polymeric chains are formed. Complex **3** is a centrosymmetric dimer, in which two $Zn^{II}$ ions are bridged by two adenine ligands coordinated by N3 and N9 atoms from a pair of head-to-tail Hade ligands to give a $\mu$-N3,N9 coordination mode. The metallo-supramolecular crystal structures of **1**−**3** are essentially maintained by hydrogen-bonding and $\pi,\pi$-stacking interactions involving the adenine, the carboxylate groups, and water molecules of coordination and crystallization (in compounds **1** and **3**). In these structures, the nature of the malonate coordination is dependent on the metal, whereas the hydrogen bonding and $\pi$-stacking capabilities of the adenine ligand influence the interactions observed in forming the three-dimensional structures. The magnetic properties of **2** were investigated in the temperature range of 2−300 K. Overall, weak antiferromagnetic behavior occurs ($J = -3$ cm$^{-1}$) with a susceptibility maximum at 50 K, with the exchange pathway provided by aqua bridges [Cu−Cu separation of 3.3522(5) Å]. Very weak ferromagnetic interactions are also observed through the malonate ligand in an uncommon anti-skew noncoplanar coordination mode, with a copper−copper separation of 5.3828(5) Å. Magnetostructural comparisons with analogous compounds with oxo-bridged Cu(II) binuclear complexes are also provided. Spectroscopic and thermal stability data for all complexes are described in detail.

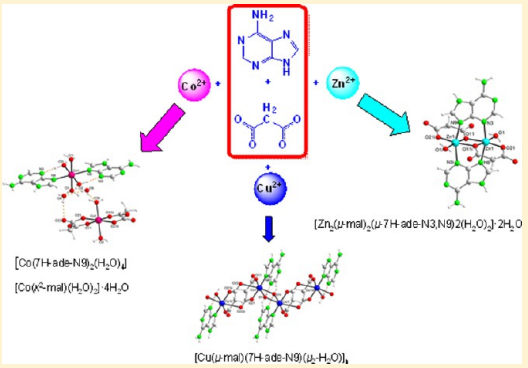


## INTRODUCTION

The successful synthesis of preconceived supramolecular assemblies depends on the careful selection of starting materials with potential for appropriate conformations and interactions (coordination, hydrogen bonding, $\pi-\pi$, C−H···$\pi$, and/or other van der Waals interactions), and of reaction conditions that effectively muster these interactions to produce the desired structure.[1−5] General principles in this field include the definition of modular units in which metal ions act as formers (rather than templates), arranging ligands around themselves in accordance with their coordination numbers and stereochemical preferences, the use of ligands with hydrogen-bonding positions that will be available for the construction of hydrogen bond networks,[6] the enrichment of such networks, to the benefit of supramolecular stability, by the additional presence of water molecules,[7] and the use of supramolecular synthons organized through specific intermolecular interactions.[8] However since both metal ions and ligands can have multiple possibilities of interaction, application of these principles requires an understanding of the factors that govern their "choice" of interaction in particular cases; the more that is known of their behavior in particular cases, the better will be that understanding.

The highly soluble nucleobase adenine (Hade) has five proton attachment sites with basicities that decrease in the order of N9 > N1 > N7 > N3(endocyclic) > N6(exocyclic). This unit provides a very wide range of binding possibilities, including monodentate, bridging, and/or chelating bidentate and tridentate modes. Which mode is realized depends essentially on its substituents, the properties of the metal ion, and the properties of any auxiliary ligands that complete the metal coordination sphere.[9]

**Received:** September 30, 2013
**Revised:** November 23, 2013
**Published:** December 4, 2013

  

**Table 1. Crystal Data and Structure Refinement for 1−3**

| compound | 1 | 2 | 3 |
|---|---|---|---|
| empirical formula | $C_{16}H_{34}Co_2N_{10}O_{18}$ | $C_8H_9CuN_5O_5$ | $C_{16}H_{22}N_{10}O_{12}Zn_2$ |
| color, habit | pink, prism | blue, needle | colorless, prism |
| formula weight | 772.39 | 318.74 | 677.18 |
| temperature (K) | 100(2) | 100(2) | 100(2) |
| crystal size (mm) | 0.16 × 0.11 × 0.08 | 0.15 × 0.08 × 0.05 | 0.35 × 0.13 × 0.13 |
| crystal system | monoclinic | monoclinic | monoclinic |
| space group | $P2_1/c$ (no. 14) | $P2_1/c$ (no. 14) | $P2_1/c$ (no. 14) |
| unit cell dimensions | | | |
| $a$ (Å) | 14.2033(8) | 9.7930(5) | 7.0521(3) |
| $b$ (Å) | 14.7848(8) | 14.4770(7) | 10.5050(3) |
| $c$ (Å) | 7.0659(3) | 7.6369(4) | 16.0669(6) |
| $\alpha$ (deg) | 90(0) | 90(0) | 90(0) |
| $\beta$ (deg) | 102.643(2) | 106.032(3) | 90.121(2) |
| $\gamma$ (deg) | 90(0) | 90(0) | 90(0) |
| volume (Å$^3$) | 1447.81(13) | 1040.60(9) | 1190.27(8) |
| $Z$ | 2 | 4 | 2 |
| density (Mg/m$^3$) | 1.772 | 2.035 | 1.889 |
| absorption coefficient (mm$^{-1}$) | 1.244 | 2.129 | 2.101 |
| $\theta$ range for data collection (deg) | 1.47 to 27.13 | 2.16 to 27.88 | 2.32 to 30.55 |
| index ranges | $-18 \le h \le 17$ | $-12 \le h \le 12$ | $-10 \le h \le 10$ |
| | $0 \le k \le 18$ | $0 \le k \le 19$ | $0 \le k \le 15$ |
| | $0 \le l \le 9$ | $0 \le l \le 10$ | $0 \le l \le 22$ |
| absorption correction | SADABS | SADABS | SADABS |
| reflections collected | 12732 | 37590 | 38925 |
| indices reflections ($R_{int}$) | 3173, 0.0526 | 2472, 0.0318 | 3633, 0.0307 |
| data/parameters | 3173/250 | 2472/187 | 3633/202 |
| final $R$ indices [$I > 2\sigma(I)$] | $R_1$ = 0.0347 | $R_1$ = 0.0252 | $R_1$ = 0.0224 |
| | $wR_2$ = 0.0807 | $wR_2$ = 0.0581 | $wR_2$ = 0.0541 |
| $R$ indices (all data) | $R_1$ = 0.0533 | $R_1$ = 0.0313 | $R_1$ = 0.0276 |
| | $wR_2$ = 0.0975 | $wR_2$ = 0.0599 | $wR_2$ = 0.0525 |
| goodness-of-fit | 1.027 | 1.061 | 1.045 |
| largest different peak/hole (eÅ$^{-3}$) | 0.361/−0.457 | 0.468/−0.383 | 0.431/−0.287 |

Carboxylate ligands have been widely used in magnetic systems due to the versatility of the carboxylate group as a bridge between metal ions that can mediate magnetic exchanges of various kinds.[10] Among the carboxylates, the malonate dianion (mal) can adopt a variety of coordination modes, including monodentate, chelating, and bridging, and more than one of these modes can occur in the same compound.[11]

As an extension of our work on the crystal engineering of inorganic−organic hybrid materials,[12] three new mixed complexes of $Co^{II}$, $Cu^{II}$, or $Zn^{II}$ with adenine (Hade) and malonic acid ($H_2$mal) ligands were isolated and fully characterized by elemental analysis, mass spectrometry, FT-IR spectroscopy, X-ray crystallography, and TG-DTG. The structures of these compounds are discussed in regard to the roles of metal ions, ligands, and weak intra- and intermolecular interactions. Additionally, the magnetic properties of the 1D coordination polymer [Cu($\mu$-mal)(7H-ade-N9)($\mu_2$-$H_2O$)] are presented.

## EXPERIMENTAL SECTION

**Materials and Physical Measurements.** All of the starting materials employed were commercially available (Hade was obtained from Acros, $H_2$mal was purchased from Aldrich, and other analytical-grade reagents were from Merck) and were used without further purification. Elemental analyses for carbon, hydrogen, and nitrogen were performed with a Fisons-Carlo Erba 1108 microanalyser. Mass spectra were obtained on a BIOTOF II API 4000 spectrometer for ESI. $^1$H NMR and $^{13}$C NMR spectra in DMSO-$d_6$ for **3** were run on Bruker AMX 300 and WM 300 instruments, respectively, using TMS as an internal reference. IR spectra were recorded as KBr pellets (4000−400 cm$^{-1}$) on a Bruker IFS-66v spectrophotometer or with a Jasco FT-IR 410 spectrophotometer. Electronic (diffuse reflectance) spectra were recorded on a Shimadzu UV-3101PC spectrophotometer. TGA experiments were carried out on a Shimadzu Thermobalance TGA-DTG-50H instrument from room temperature to 800 °C in a flow of air (100 mL min$^{-1}$) and series of FT-IR spectra (20−30 per sample) of evolved gases were recorded using a coupled FT-IR Nicolet Magma 550 spectrophotometer. X-band electron paramagnetic resonance spectra at room temperature were recorded on a Bruker EPR 300E spectrometer. Room temperature magnetic moments were determined for **1** on a Quantum Design PPMS susceptometer. Variable temperature magnetic susceptibility measurements were carried out on polycrystalline samples of **2** in the temperature range of 2−300 K using a Quantum Design SQUID susceptometer under a magnetic field of 1 T. Diamagnetic corrections for the complexes were estimated from Pascal's constants.

**Synthesis of the Complexes.** *Synthesis of [Co(Hade)$_2$(H$_2$O)$_4$]-[Co(mal)$_2$(H$_2$O)$_2$]·4H$_2$O (**1**).* $Co(NO_3)_2{\cdot}6H_2O$ (290 mg, 1 mmol), $H_2$mal (110 mg, 1 mmol), and NaOH (80 mg, 2 mmol) were reacted in water (100 mL) with stirring and Hade (140 mg, 1 mmol) was added with heating (50−60 °C) and stirring until dissolution was complete. The cloudy solution was filtered, and a pink solid was isolated. Slow evaporation of the mother liquors provided suitable crystals for X-ray diffraction. Yield = 55% based on $Co^{II}$ salt.

Elemental analysis. Found: C, 25.04; H, 4.64; N, 18.36. Calcd for $C_{16}H_{34}Co_2N_{10}O_{18}$ (772.39): C, 24.88; H, 4.43; N, 18.13. IR ($\nu_{max}$/cm$^{-1}$): 3473s $\nu$(OH); 3354s, 3146s $\nu$(NH); 1656s $\delta(NH_2)$; 1632s


dx.doi.org/10.1021/cg401455c | Cryst. Growth Des. 2014, 14, 249−260

$\nu$(CN) + $\delta$(NH); 1584vs, 1571vs $\nu_{asym}$(COO); 1466m, 1436m, 1408m $\nu$(CN) + $\nu$(CC); 1364s, 1336m $\nu_{sym}$(COO); 1264w $\nu$(CN); 1185w, 1043w $\nu$(CN), 967w, 923w $\rho(NH_2)$; 797w, 721m $\delta$(OCO); 608m, 546w, 465w, 454w $\nu$(CoO); 392m, 383m, 374m, 324s $\nu$(CoN); 239s, 215s. ESI MS, $m/z$ (% $I_{rel}$): 293.88 (100), [Co(mal)(ade) − H)]$^+$; 368.87 (44), [Co(Hade)(Hmal)$_2$)]$^+$. UV/vis ($\lambda_{max}$, cm$^{-1}$): 29070, 20920, 15106. $\mu$ = 3.47$\mu_B$.

*Synthesis of [Cu(mal)(Hade)(H$_2$O)]$_n$ (**2**).* $Cu_2CO_3(OH)_2$ (110 mg, 0.5 mmol) and $H_2$mal (110 mg, 1 mmol) were reacted in water (100 mL) in a Kitasato flask with heating (50−60 °C), stirring, and vacuum until complete dissolution was achieved. Hade (140 mg, 1 mmol) was added, and the mixture was stirred for 30 min. The cloudy solution was filtered and cooled to room temperature. After a week of evaporation, dark blue crystals had formed and many of these were suitable for X-ray diffraction studies. The product was collected in successive fractions. Yield = 70% based on $Cu^{II}$ salt.

Elemental analysis. Found: C, 29.97; H, 2.99; N, 21.65. Calcd for $C_8H_9CuN_5O_5$ (318.75): C, 30.15; H, 2.85; N, 21.97. IR ($\nu_{max}$/cm$^{-1}$): 3453bm, $\nu$(OH); 3361s, 3172s $\nu$(NH); 3109s, 1675vs $\delta(NH_2)$; 1614s $\nu$(CN) + $\delta$(NH); 1585vs $\nu_{asym}$(COO); 1453s, 1400s $\nu$(CN) + $\nu$(CC); 1370m, 1353m $\nu_{sym}$(COO); 1329m, 1280m $\nu$(CN); 1210m, 1107w, 1019w $\nu$(CN); 983w, 954w $\rho(NH_2)$; 909w, 789m, 736m, 726m $\delta$(OCO); 691w, 661m, 623w, 608m, 561vw, 553w, 482w, 465vw, 422vw $\nu$(CuO), 376w, 323w, 305w, 208w. ESI MS, $m/z$ (% $I_{rel}$): 300.99 (7), [Cu(mal)(Hade)$^+$; 318.86 (4) [Cu(mal)(Hade)(H$_2$O)], 333.04 (14), [Cu(Hade)$_2$]$^+$. UV−vis ($\lambda_{max}$, cm$^{-1}$): 30100, 15038.

*Synthesis of [Zn(mal)(Hade)(H$_2$O)]$_2$·2H$_2$O (**3**).* $Zn_2CO_3(OH)_2$ (230 mg, 1 mmol) and $H_2$mal (210 mg, 2 mmol) were reacted in water (100 mL) in a Kitasato flask with heating (50−60 °C), stirring, and vacuuming. The solution was left to cool to room temperature and Hade (270 mg, 2 mmol) was added with stirring. The mixture was stirred for two days. The cloudy solution was filtered, and slow evaporation of the solution gave a small amount of crystals suitable for X-ray analysis. The product was collected in successive fractions. Yield 77% on the basis of $Zn^{II}$ salt.

Elemental analysis. Found: C, 27.35; H, 2.61; N, 21.00. Calcd for $C_{16}H_{22}N_{10}O_{12}Zn_2$ (677.22): C, 28.38; H, 3.27; N, 20.68. $^1$H NMR (DMSO-$d_6$, ppm): 12.82 (1H, bs, N7H), 8.09 (1H, s, C2H), 8.07 (1H, s, C8H); 7.06 (2H, s, N6H$_2$); 2.98 (2H, s, CH$_2$). $^{13}$C NMR (DMSO-$d_6$, ppm): 170.0 CO, 156.2 C6, 152.3 C1, 138.9 C5, 131.7 C8, 125.3 C4, 38.9 CH$_2$. IR ($\nu_{max}$/cm$^{-1}$): 3425s $\nu$(OH); 3340s, 3194m $\nu$(NH); 1681s $\delta(NH_2)$; 1653s, 1623vs, 1600vs $\nu$(CN) + $\delta$(NH); 1564vs $\nu_{asym}$(COO); 1473m, 1430m, 1405s $\nu$(CN) + $\nu$(CC); 1383s, 1367s, 1338m $\nu_{sym}$(COO); 1283m, 1261m $\nu$(CN); 1219m, 1155m, 1130w, 1035w $\nu$(CN); 962m $\rho(NH_2)$; 938w, 795m, 724m $\delta$(OCO); 668m, 647m, 610m, 486w, 475w, 466w, 427w $\nu$(ZnO), 337w, 240w, 218w. ESI MS, $m/z$ % $I_{rel}$): 266.08 (28), [Zn$_2$(Hade)]$^+$; 301.12 (59), [Zn(mal)(ade)]$^+$; 331.02 (98), [Zn(ade)$_2$ − 2H]$^+$; 437.20 (23), [Zn(mal)(Hade)$_2$]$^+$.

**Crystallography.** Diffraction data were obtained at room temperature on a Bruker X8 KappaAPEXII[13] from crystals mounted on glass fibers. Data were corrected for Lorentz and polarization effects and for absorption following the SADABS method.[14] The structures were solved by direct methods,[15] which revealed the positions of all nonhydrogen atoms. These were refined on $F^2$ by a full-matrix least-squares procedure using anisotropic displacement parameters.[15] All hydrogen atoms were located in difference maps, and the positions of O−H and N−H hydrogens were refined (others were included as riders); the isotropic displacement parameters of H atoms were constrained to 1.2$U_{eq}$ of the carrier atoms. Molecular graphics were generated with PLATON[16] and DIAMOND.[17] The crystal data, experimental details and refinement results are summarized in Table 1.

## RESULTS AND DISCUSSION

**General Comments on Synthesis.** Reactions of Co(NO$_3$)$_2$·6H$_2$O, $Cu_2CO_3(HO)_2$, or $Zn_2CO_3(OH)_2$ with malonic acid ($H_2$mal) in basic aqueous media, followed by addition of adenine (Hade) in 1:1:1, 1:2:2, and 1:2:2 ratios, respectively, with mild heating afforded crystalline solids of formulas [Co(7H-ade-N9)$_2$(H$_2$O)$_4$][Co($\kappa^2$-mal)(H$_2$O)$_2$]·4H$_2$O (**1**), $_\infty^1$[Cu($\mu$-mal)(7H-ade-N9)($\mu_2$-H$_2$O)] (**2**), and [Zn$_2$($\mu$-mal)$_2$($\mu$-7H-ade-N3,N9)$_2$(H$_2$O)$_2$]·2H$_2$O (**3**) in good yields (see Scheme 1). The formation of these complexes was

**Scheme 1. Summary of the Conditions for the Preparation of 1−3**

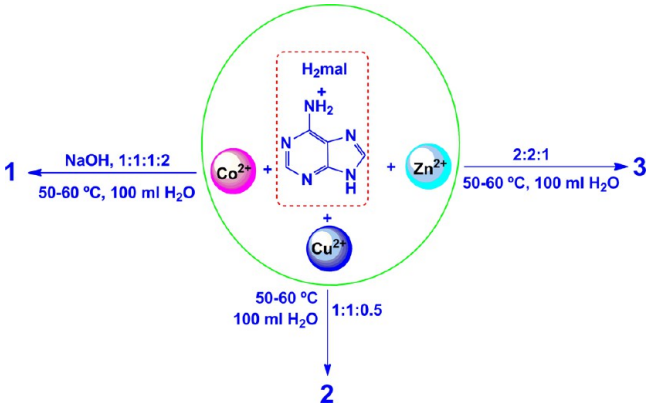


established by chemical analysis, and the presence of appropriate peaks in the electrospray ionization mass spectra (ESI-MS) at $m/z$ 293.88 [Co(mal)(ade) − H)]$^+$, 368.87 [Co(Hmal)$_2$(Hade)]$^+$, 300.99 [Cu(mal)(Hade)]$^+$, 318.86 [Cu(mal)(Hade)(H$_2$O)]$^+$, 333.04 [Cu(Hade)$_2$]$^+$, 266.08 [Zn$_2$(Hade)]$^+$, 301.12 [Zn(mal)(ade)]$^+$, 331.02 [Zn(ade)$_2$ − 2H]$^+$, and 437.20 [Zn(mal)(Hade)$_2$]$^+$.

**Structural Studies of [Co(7H-ade-N9)$_2$(H$_2$O)$_4$][Co($\kappa^2$-mal)(H$_2$O)$_2$]·4H$_2$O, 1.** Compound **1** is an ionic complex consisting of a [Co(7H-ade-N9)$_2$(H$_2$O)$_4$]$^{2+}$ cation that is charge-balanced by a [Co($\kappa^2$-mal)(H$_2$O)$_2$]$^{2-}$ anion and four solvent water molecules. In the cationic and anionic complexes, each cobalt atom occupies a special position (inversion center) such that there are two independent half cations and half anions in the asymmetric unit. $Co^{2+}$ in the cation has an undistorted octahedral geometry, with four oxygen atoms of aqua ligands in the equatorial positions and two trans N9 atoms of the neutral adenine achieving the octahedral environment around cobalt. In the [Co($\kappa^2$-mal)(H$_2$O)$_2$]$^{2-}$ anion, four coplanar oxygen atoms from two chelated malonate ligands provide the equatorial plane, and the axial positions are occupied by two aqua ligands. Selected bond lengths and angles are given in Tables 2 and 3, and a representation of the two ions is shown in Figure 1.

In the anion, the average Co−O distance in the equatorial plane is 2.069 Å. This value is consistent with the general coordination rules and is in good agreement with those observed in transition metal complexes containing the monomeric building block [M($\kappa^2$-mal)(H$_2$O)$_2$]$^{2-}$ anion.[11b,18] As expected, the apical Co−O length of 2.127 Å is slightly longer than the equatorial Co−O distances and is also longer than corresponding distances reported for octahedral aquacobalt(II) complexes.[19] In the cation, the Co−N9 distance of 2.151(2) Å is comparable with the average value of 2.156(3) Å reported for cobalt complexes of adenine involving the apical N9 coordination.[20] The mean value for the equatorial Co−O bonds of 2.104(2) Å can also be considered as normal. There is an intramolecular hydrogen bond between the coordinated O2 water molecule as a hydrogen donor and the pyridine N3 atom as an acceptor (Figure 1 and Table 4). These interactions


dx.doi.org/10.1021/cg401455c | Cryst. Growth Des. 2014, 14, 249−260

**Table 2. Selected Bond Lengths (Å) for Compounds 1−3**

| | | | |
|---|---|---|---|
| compound **1** | | | |
| Co(1)−O(1) | 2.0913(18) | Co(2)−O(21) | 2.0531(16) |
| Co(1)−O(2) | 2.1113(17) | Co(2)−O(11) | 2.0847(16) |
| Co(1)−N(9) | 2.1514(19) | Co(2)−O(3) | 2.1252(17) |
| Co(1)···Co(2)[a] | 8.5964(4) | | |
| compound **2** | | | |
| Cu(1)−O(11) | 1.9067(14) | Cu(1)−O(22) | 2.7949(15) |
| Cu(1)−O(21) | 1.9345(13) | Cu(1)···Cu(1)[b] | 3.3523(5) |
| Cu(1)−O(1) | 1.9611(14) | Cu(1)···Cu(1)[c] | 5.3828(5) |
| Cu(1)−N(9) | 2.0078(15) | O(1)···O(1)[b] | 2.972(3) |
| Cu(1)−O(1)[b] | 2.4881(15) | | |
| compound **3** | | | |
| Zn(1)−O(21) | 2.0276(10) | Zn(1)−O(11) | 2.1516(9) |
| Zn(1)−O(11)[d] | 2.0842(9) | Zn(1)−N(3) | 2.1401(11) |
| Zn(1)−O(1) | 2.0692(10) | Zn(1)···Zn(1)[d] | 3.1135(3) |
| Zn(1)−N(9) | 2.1594(11) | O(11)···O(11)[d] | 2.8729(18) |

[a]For compound 1, symmetry transformations of i: $-x + 1, -y, -z$. [b]For compound 2, symmetry transformations of i: $-x, -y, -z - 1$. [c]For compound 2, symmetry transformations of ii: $-x, -y, -z - 1$. [d]For compound 3, symmetry transformations i: $-x, -y, -z - 1$.

contribute to stabilize the cation, resulting in a slight increase in the Co−O distances and a decrease in the Co−N distances.

The $[Co(7H\text{-ade-}N9)_2(H_2O)_4]^{2+}$ cations are interconnected through hydrogen bonding between the aqua ligand O2 and the uncoordinated pyridine nitrogen atom N1 of the adenine (Table 4). These hydrogen bonds lead to zigzag steps that form sheets, as shown in Figure 2 (see SM1 of the Supporting Information).

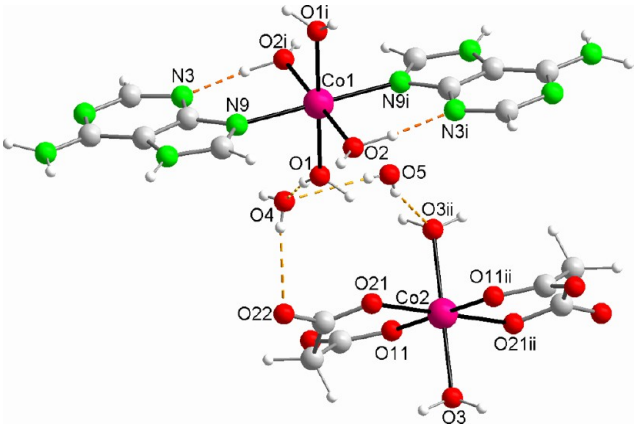


**Figure 1.** Molecular structure of **1** showing the hydrogen-bonding interactions between cation and anion (orange dashed lines). Symmetry codes: (i) $-x + 1, -y, -z$ and (ii) $-x, -y, -z + 1$.

As for the cations, hydrogen bonds also interconnect the $[Co(\kappa^2\text{-mal})(H_2O)_2]^{2-}$ anions and this leads to the formation of sheets, as shown in Figure 3. These hydrogen bonds involve the aqua ligand O3 as hydrogen donors and the uncoordinated malonate oxygen atom O12 as acceptors, so that each anion is connected simultaneously to four neighboring anions by hydrogen bonding, two as acceptors and two as donors. In addition, each anion is linked to the crystallization water molecules to generate ten-membered hydrogen-bonded rings with the graph set $R_3^3(10)$[21] (Figure 1). This assembly is attached to the corresponding cation by hydrogen bonding between the aqua ligand O1 as a donor and the crystallization water molecule O4 as an acceptor (Figure 1).

**Table 3. Selected Bond Angles (deg) for the Complexes 1−3**

| | | | |
|---|---|---|---|
| compound **1** | | | |
| O(1)−Co(1)−O(2)[a] | 90.26(7) | O(21)−Co(2)−O(11)[b] | 92.66(6) |
| O(1)−Co(1)−O(2) | 89.74(7) | O(21)−Co(2)−O(11) | 87.34(6) |
| O(1)−Co(1)−N(9)[a] | 90.54(7) | O(21)−Co(2)−O(3) | 92.81(7) |
| O(2)−Co(1)−N(9)[a] | 90.09(7) | O(11)−Co(2)−O(3) | 95.68(7) |
| O(1)−Co(1)−N(9) | 89.46(7) | O(21)−Co(2)−O(3)[b] | 87.19(7) |
| O(2)−Co(1)−N(9) | 89.91(7) | O(11)−Co(2)−O(3)[b] | 84.32(7) |
| compound **2** | | | |
| O(11)−Cu(1)−O(21) | 95.03(6) | O(1)−Cu(1)−O(1)[c] | 82.93(5) |
| O(11)−Cu(1)−O(1) | 170.89(6) | N(9)−Cu(1)−O(1)[c] | 98.52(6) |
| O(21)−Cu(1)−O(1) | 87.29(6) | O(11)−Cu(1)−O(22) | 88.96(5) |
| O(11)−Cu(1)−N(9) | 88.16(6) | O(21)−Cu(1)−O(22) | 80.62(5) |
| O(21)−Cu(1)−N(9) | 173.31(6) | O(1)−Cu(1)−O(22) | 100.11(5) |
| O(1)−Cu(1)−N(9) | 90.48(6) | N(9)−Cu(1)−O(22) | 93.58(5) |
| O(11)−Cu(1)−O(1)[c] | 88.37(5) | O(1)[c]−Cu(1)−O(22) | 167.52(4) |
| O(21)−Cu(1)−O(1)[c] | 87.47(5) | Cu(1)−O(1)−Cu(1)[c] | 97.03(5) |
| compound **3** | | | |
| O(21)−Zn(1)−O(11)[d] | 89.38(4) | O(1)−Zn(1)−O(11) | 93.22(4) |
| O(21)−Zn(1)−O(1) | 92.57(4) | N(9)−Zn(1)−O(11) | 81.15(4) |
| O(11)[d] −Zn(1)−O(1) | 174.32(4) | O(21)−Zn(1)−N(3) | 101.02(4) |
| O(21)−Zn(1)−N(9) | 92.25(4) | O(11)[d]−Zn(1)−N(3) | 84.24(4) |
| O(11)[d]−Zn(1)−N(9) | 84.09(4) | O(1)−Zn(1)−N(3) | 90.15(4) |
| O(1)−Zn(1)−N(9) | 101.16(4) | N(9)−Zn(1)−N(3) | 162.20(4) |
| O(21)−Zn(1)−O(11) | 171.96(4) | O(11)−Zn(1)−N(3) | 84.55(4) |
| O(11)[d]−Zn(1)−O(11) | 85.39(4) | Zn(1)[d]−O(11)−Zn(1) | 94.61(4) |

[a]For compound 1, symmetry transformations of i: $-x + 1, -y, -z$. [b]For compound 1, symmetry transformations of ii: $-x,-y, -z + 1$. [c]For compound 2, symmetry transformations of i: $-x, -y, -z$. [d]For compound 3, symmetry transformations of i: $-x, -y, -z + 1$.


dx.doi.org/10.1021/cg401455c | Cryst. Growth Des. 2014, 14, 249−260

Table 4. Hydrogen Bonds (Å, deg) for Compounds 1−3

| D−H···A | d(D−H) | d(H···A) | d(D···A) | ∠(DHA) |
|---|---|---|---|---|
| compound **1** | | | | |
| O(1)−H(1A)···O(4) | 0.82(3) | 1.98(3) | 2.794(3) | 170(3) |
| O(1)−H(1B)···N(1)[c] | 0.88(3) | 1.88(3) | 2.745(3) | 167(3) |
| O(2)−H(2A)···O(22)[d] | 0.80(3) | 2.05(3) | 2.843(2) | 169(3) |
| O(2)−H(2B)···N(3)[a] | 0.82(3) | 1.88(3) | 2.640(3) | 155(3) |
| N(7)−H(7A)···O(11)[e] | 0.79(3) | 2.06(3) | 2.852(3) | 173(3) |
| N(10)−H(10A)···O(5)[f] | 0.81(3) | 2.11(3) | 2.899(3) | 165(3) |
| N(10)−H(10B)···O(12)[e] | 0.81(3) | 2.03(3) | 2.807(3) | 159(3) |
| O(3)−H(3A)···O(12)[g] | 0.83(3) | 1.98(3) | 2.785(2) | 166(3) |
| O(3)−H(3B)···O(5)[h] | 0.86(3) | 1.93(3) | 2.766(3) | 163(3) |
| O(4)−H(4A)···O(22) | 0.85(3) | 1.99(3) | 2.831(3) | 170(3) |
| O(4)−H(4B)···O(22)[f] | 0.69(3) | 2.09(3) | 2.775(2) | 175(4) |
| O(5)−H(5A)···O(4) | 0.74(3) | 2.01(3) | 2.751(3) | 179(3) |
| O(5)−H(5B)···O(3)[b] | 0.88(3) | 2.10(3) | 2.870(3) | 145(3) |
| compound **2** | | | | |
| O(1)−H(1A)···O(12)[j] | 0.76(3) | 1.84(3) | 2.589(2) | 168(3) |
| O(1)−H(1B)···N(3) | 0.75(3) | 1.91(3) | 2.624(2) | 163(3) |
| N(7)−H(7)···O(22)[k] | 0.80(2) | 1.99(2) | 2.755(2) | 158(2) |
| N(10)−H(10A)···O(12)[l] | 0.80(3) | 2.06(3) | 2.803(2) | 154(2) |
| N(10)−H(10B)···O(21)[k] | 0.82(3) | 2.47(3) | 3.159(2) | 143(2) |
| N(10)−H(10B)···O(22)[k] | 0.82(3) | 2.30(3) | 3.086(2) | 162(2) |
| compound **3** | | | | |
| O(1)−H(1A)···O(2)[m] | 0.80(2) | 1.92(2) | 2.719(2) | 175(2) |
| O(1)−H(1B)···O(12) | 0.76(2) | 2.05(2) | 2.767(1) | 157(2) |
| N(7)−H(7A)···O(21)[n] | 0.89(2) | 1.86(2) | 2.748(2) | 173(2) |
| N(10)−H(10A)···O(22)[n] | 0.84(2) | 2.04(2) | 2.864(2) | 170(2) |
| N(10)−H(10B)···O(12)[o] | 0.85(2) | 2.09(2) | 2.869(2) | 152(2) |
| O(2)−H(2A)···O(22) | 0.79(2) | 1.97(2) | 2.756(2) | 170(2) |
| O(2)−H(2B)···N(1) [p] | 0.80(2) | 2.09(2) | 2.867(2) | 165(2) |

[a]For compound 1, symmetry transformations of i: $-x+1, -y, -z$. [b]For compound 1, symmetry transformations of ii: $-x, -y, -z+1$. [c]For compound 1, symmetry transformations of iii: $-x+1, y-1/2, -z+1/2$. [d]For compound 1, symmetry transformations of iv: $-x+1, -y, -z+1$. [e]For compound 1, symmetry transformations of v: $x+1, y, z$. [f]For compound 1, symmetry transformations of vi: $-x+1, y+1/2, -z+1/2$. [g]For compound 1, symmetry transformations of vii: $-x, y-1/2, -z+3/2$. [h]For compound 1, symmetry transformations of viii: $x, y, z+1$. [I]For compound 1, symmetry transformations of ix: $x, -y+1/2, z-1/2$. [j]For compound 2, symmetry transformations of iii: $-x, y+1/2, -z-1/2$. [k]For compound 2, symmetry transformations of iv: $x+1, y, z+1$. [l]For compound 2, symmetry transformations of v: $-x+1, y+1/2, -z+1/2$. [m]For compound 3, symmetry transformations of ii: $x-1, y, z$. [n]For compound 3, symmetry transformations of iii: $x, -y+1/2, z+1/2$ [o]For compound 3, symmetry transformations of iv: $-x, -y+1, -z+1$. [p]For compound 3, symmetry transformations of v: $-x+1, y-1/2, -z+1/2$.

The most important supramolecular interactions in the crystal structure of **1** are those between the cations and anions (Figure 4). The three NH groups of each of the Hade ligands form hydrogen bonds with oxygen atoms of a crystallization water molecule O5 and with a neighboring anion. The imidazole NH bonds and an amino NH bond form a heterosynthon with a carboxylate group to generate 9-membered hydrogen-bonded rings with the graph set $R_2^2(9)$. This ring is fused to another ring, with the graph set $R_4^2(8)$, that bridges two different ions and is formed by the amino group of a cation and the aqua ligand of an anion as donors and the uncoordinated oxygen atoms of a carboxylate of a new neighbor anion and the crystallization water molecule O5 as acceptors. Additionally, $R_2^2(12)$ ring motifs are fused to $R_2^2(9)$ with aqua and carboxylate oxygen atoms as donors and acceptors, respectively, in addition to the aforementioned N−H···O shared by both rings. Note that the H bonds to the malonate carboxylate groups are likely to be very strong because of the negative charge of the latter.[22] Details of the hydrogen bond parameters for compound **1** are given in Table 4.

Finally, the cationic chain (Figure 2) is linked by $\pi-\pi$ stacking interactions between overlapping Hade units along the *c* axis at a centroid−centroid distance[23] of around 3.5 Å (see Figure SM5 of the Supporting Information). Analysis of the columnar arrays and the relationships between neighboring ring cations in stacks shows that a zigzag array is present (see SM2 of the Supporting Information). Intermolecular interactions between cations along the columns and between adjacent columns are reinforced by the hydrogen-bonding interactions described above (see SM1 of the Supporting Information).

**Structural Studies of $_\infty^1$[Cu($\mu$-mal)(7H-ade-N9)($\mu_2$-H$_2$O)], 2.** The structure determination revealed that the binuclear [Cu(mal)(Hade)(H$_2$O)]$_2$ units of **2** are bridged by malonate ligands with the formation of 1D coordination polymeric chains along the *c* axis, as shown in Figure 5. Selected bond lengths and angles are given in Tables 2 and 3. The coordination environment around each copper ion may be described as pseudo-octahedral. The equatorial plane contains two oxygen atoms (O11 and O21) of the chelated malonate, one oxygen atom (O1) of an asymmetrically bridging water molecule and one nitrogen atom (N9) of the adenine ligand. All four of these bonds are short. The oxygen atom (O22) of a carboxylate group of the malonate ligand from a neighboring mal$^{2-}$ and the symmetry related oxygen atom O1$^{i}$ (i = −x, −y, −z) from a second bridging water molecule occupy the axial positions and both have long bonds (Table 2). The coordination may be considered as 4 + 1 + 1, as usually found in Jahn−Teller active copper(II) complexes. Deviations of the copper atoms from the mean plane formed by the four equatorial atoms is about 0.022(7) Å, and the maximum deviation of any equatorial atom form the mean plane around copper is 0.1289(7) Å. The dihedral angle between the equatorial plane and the mean plane of adenine is 10.86(7) Å.

The adenine is coordinated via N9 with a Cu−N distance of 2.008(2) Å (Table 2), as found in other octahedral copper(II) complexes with purine or adenine as terminal ligands.[24]

A di-$\mu$-aqua-dicopper(II) motif is formed by two symmetry-related copper atoms. The bridging oxygen atoms arrange to form a planar central Cu$_2$O$_2$ rhombus with O1−Cu1−O1$^{i}$ and Cu1−O1−Cu1$^{i}$ bond angles of 82.97(5)° and 97.03(5)°, respectively. The Cu−$\mu$−OH$_2$ distances found in the complex lie in the range found in six-coordinate polymeric copper(II) compounds (i.e., 1.91 to 1.99 Å for Cu−O$_{equatorial}$ and 2.37 to 2.99 Å for Cu−O$_{apical}$).[25] In this motif, the Cu1−Cu1$^{i}$ distance is 3.3522(5) Å.

In contrast to the situation found in **1**, the malonate in **2** acts as a tridentate ligand. In this coordination mode, two oxygen atoms (O11 and O21) coordinate the same metal in a $\eta^5$-chelation [Cu−O, 1.907(1), and 1.934(1) Å, respectively] and another one is bound to an additional metal as a unidentate ligand [Cu1−O22 2.795(2) Å], adopting a bridging $\kappa^2$O,O″;$\kappa$O′ coordination mode typical of malonate complexes.[11a] The remaining oxygen atoms act as hydrogen bond acceptors, and this blocks polymerization in this direction.

The most interesting structural feature in complex **2** is that each copper(II) ion in the dimeric subunit is linked to two


dx.doi.org/10.1021/cg401455c | Cryst. Growth Des. 2014, 14, 249−260

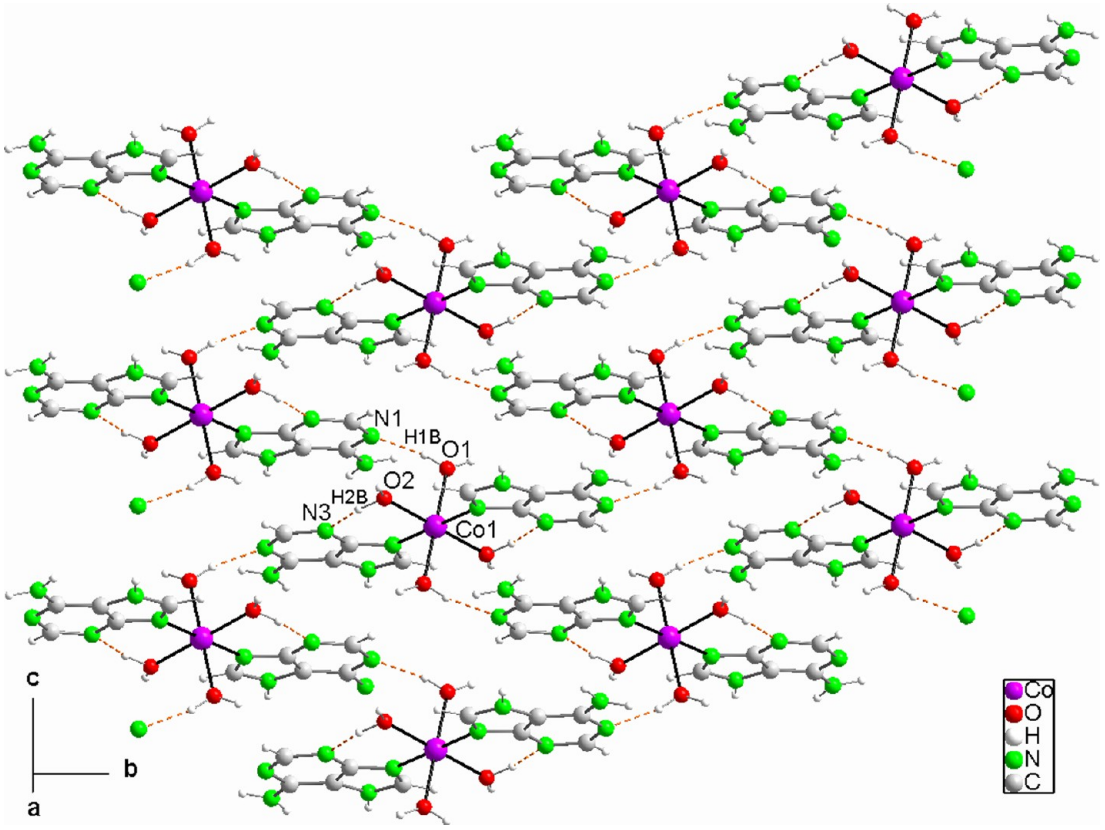


**Figure 2.** Hydrogen-bonded sheets interconnecting the complex cation in the structure of **1**. Hydrogen bonds are shown as orange dashed lines.

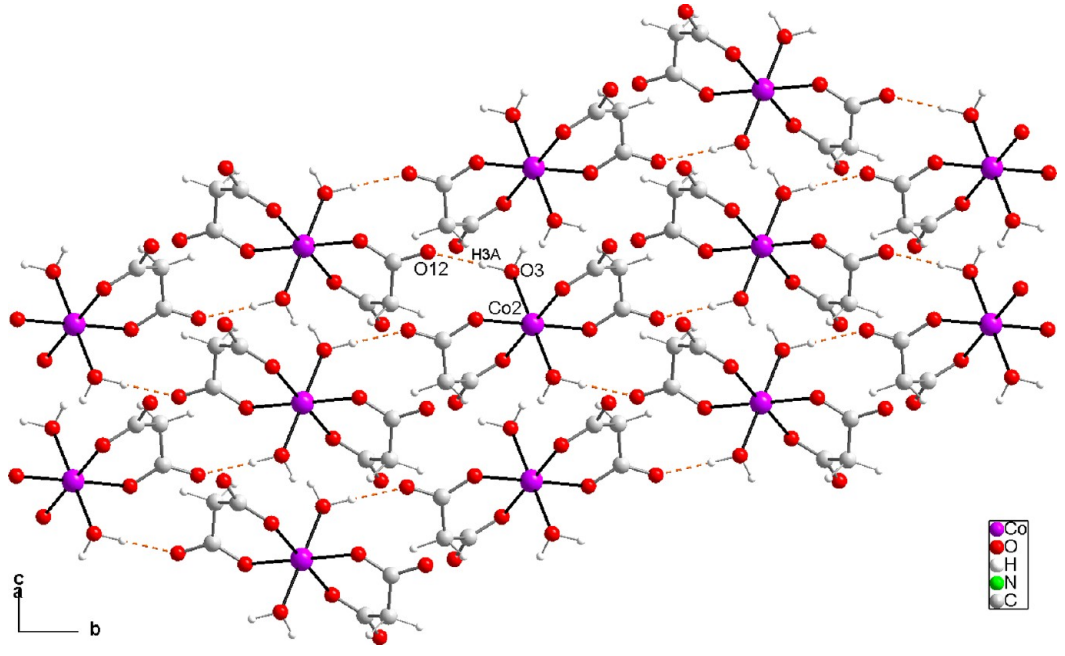


**Figure 3.** Layers of hydrogen-bonded interconnecting anions in the structure of **1**. Hydrogen bonds are shown as orange dashed lines.

copper(II) ions in two adjacent dimeric subunits by two carboxylate groups in an uncommon *anti-skew* noncoplanar coordination mode (torsion angles Cu−O−C−O *ca.* 90° and 172°). This leads to eight-membered metallocycles with a *twist-chair* conformation[26] and a Cu1−Cu1$^{ii}$ distance of 5.3828(5) Å (ii = -x, -y, -z-1). Thus, the structure of **2** consists of zigzag chains of alternating aqua- and carboxylate-bridged copper(II) ions running along the *c* direction (Figure 5).

A packing view of **2** in the *bc* plane shows that chains are grouped together in layers through hydrogen bonding (Table 4) that involves the coordinated water and adenine molecules as donors through the O−H and N−H bonds, respectively, and coordinated and uncoordinated malonate oxygen atoms as


dx.doi.org/10.1021/cg401455c | *Cryst. Growth Des.* 2014, 14, 249−260

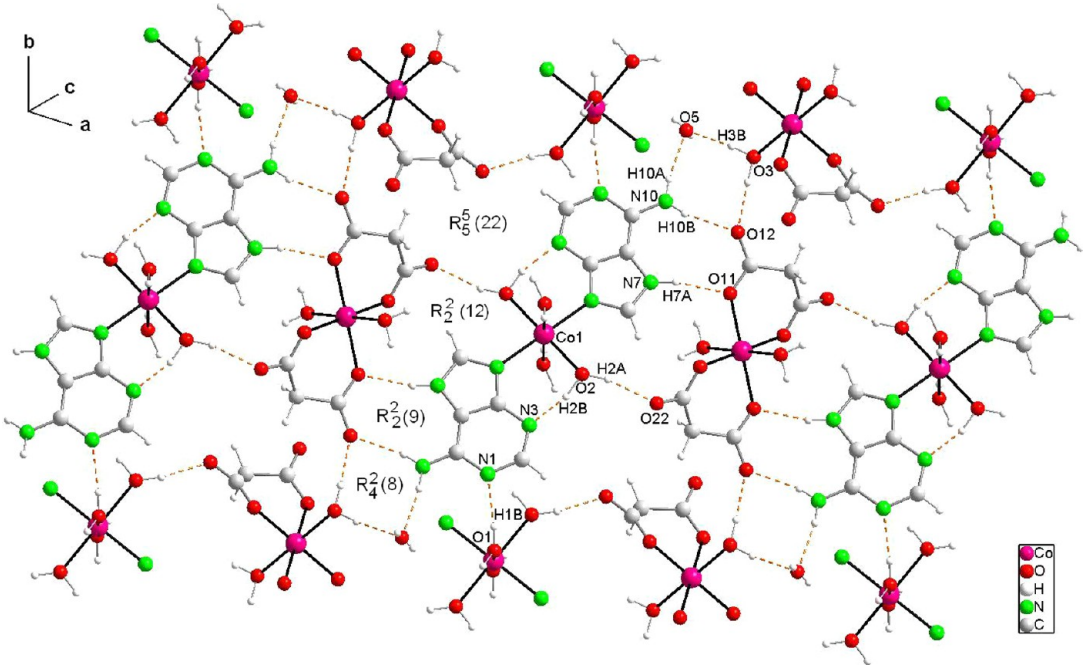


**Figure 4.** Portion of the packing diagram in **1** showing the interaction linking the cations and anions. Hydrogen bonds are shown as orange dashed lines.

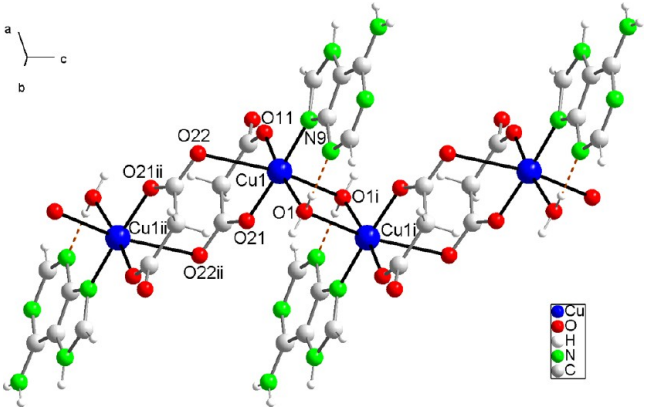


**Figure 5.** 1D coordination polymer of **2** showing the intermolecular hydrogen-bonding interactions (orange dashed lines). Symmetry codes: (i) $-x, -y, -z$; (ii) $-x, -y, -z-1$; (iii) $x, y, z+1$.

acceptors. This arrangement generates various-membered hydrogen-bonded fused rings, with the graph sets $R_3^2(8)$, $R_2^1(4)$, and $R_2^1(7)$ in the [001] direction and $R_3^4(22)$ in the [010] direction (Figure 6) to form an infinite three-dimensional network based on wavy layers, as shown in Figure 7. In addition, the layers are pillared through the adenine ligands, which are stacked through $\pi-\pi$ interactions involving the imidazole rings from adjacent chains $(-x+1, -y, -z+1)$.[23] The separation between centroids is 3.594(1) Å and the offset angle is 0° (see SM3 of the Supporting Information SM3).

**Structural Studies of $[Zn_2(\mu\text{-mal})_2(\mu\text{-7H-ade-N3,N9})_2(H_2O)_2]\cdot 2H_2O$, 3.** The structure of **3** is isotypic with $[M_2(\mu\text{-mal})_2(\mu\text{-Hade})_2(H_2O)_2]\cdot 2H_2O$ (M = Co, Ni).[11b] The structure of the main component of these compounds $[Zn(\mu_2\text{-mal})(\mu_2\text{-7H-ade-N3,N9})(H_2O)]_2$ is shown in Figure 8. This unit consists of a centrosymmetric dimer in which two zinc(II) ions are bridged by two adenine ligands coordinated by their two N atoms (pyrimidine N3 and imidazole N9) from a pair of head-to-tail arranged Hade units to give a $\mu-\kappa$N3:$\kappa$N9 coordination mode and two carboxylate oxygen atoms of two malonate dianions, each of which is also chelated to a metal center. The distorted octahedral coordination polyhedron is completed by one aqua ligand. Selected bond lengths and angles are given in Tables 2 and 3. The Zn−N bond lengths are in the range 2.14−2.16 Å, and these are longer than the Zn−$N_{(imidazole)}$ (av 2.084 Å) and Zn−$N_{(pyrimidine)}$ (av 2.065 Å) distances[27] and also longer than those in three known related binuclear zinc-$\mu$-adenine complexes.[28] It is noteworthy that in this dimer the Zn−N3 distance is shorter than the Zn−N9 distance, an effect also observed in other dinuclear zinc(II) complexes with a Hade bridge[28b] but opposite to that found in most six-coordinate dimers of divalent metal ions of the first row transition.[11b,12,29] This phenomenon is attributed to the large amount of *s* character in the coordination orbital of the imidazole nitrogen, N9.[30]

The malonate ligand links the two zinc centers to form the dimer in a tridentate $\kappa^2$O,O″:$\kappa$O coordination mode, where an oxygen atom of each carboxylate group coordinates to same metal [Zn−O: 2.1594(11) and 2.0274(10) Å] and one of them is also bound to the second metal in a bidentante manner to form an asymmetric bridge. The remaining oxygen atoms may act as hydrogen bond acceptors.

In the dinuclear units, the dihedral angle between the mean plane of the $Zn_2O_2$ unit and the adenine is ca. 90°, with Zn1···Zn1$^i$ and O11···O11$^i$ (i: $-x, -y, -z+1$) distances of 3.1135(3) and 2.876(2) Å, respectively. The observed value for the Zn···Zn separation is greater than the sum of the van der Waals radii (2.78 Å), and this strongly suggests that a direct zinc−zinc bond interaction is not present in this structure.

The crystal structure of **3** is stabilized through intermolecular hydrogen bonding involving the coordinated and uncoordinated oxygen atoms of the malonate ligand as acceptors (except O11) and N−H adenine bonds and water molecules as donors. The dimeric molecules are connected to give layers parallel to the (100) plane through N−H···O hydrogen bonds (see Figure


dx.doi.org/10.1021/cg401455c | *Cryst. Growth Des.* 2014, 14, 249−260

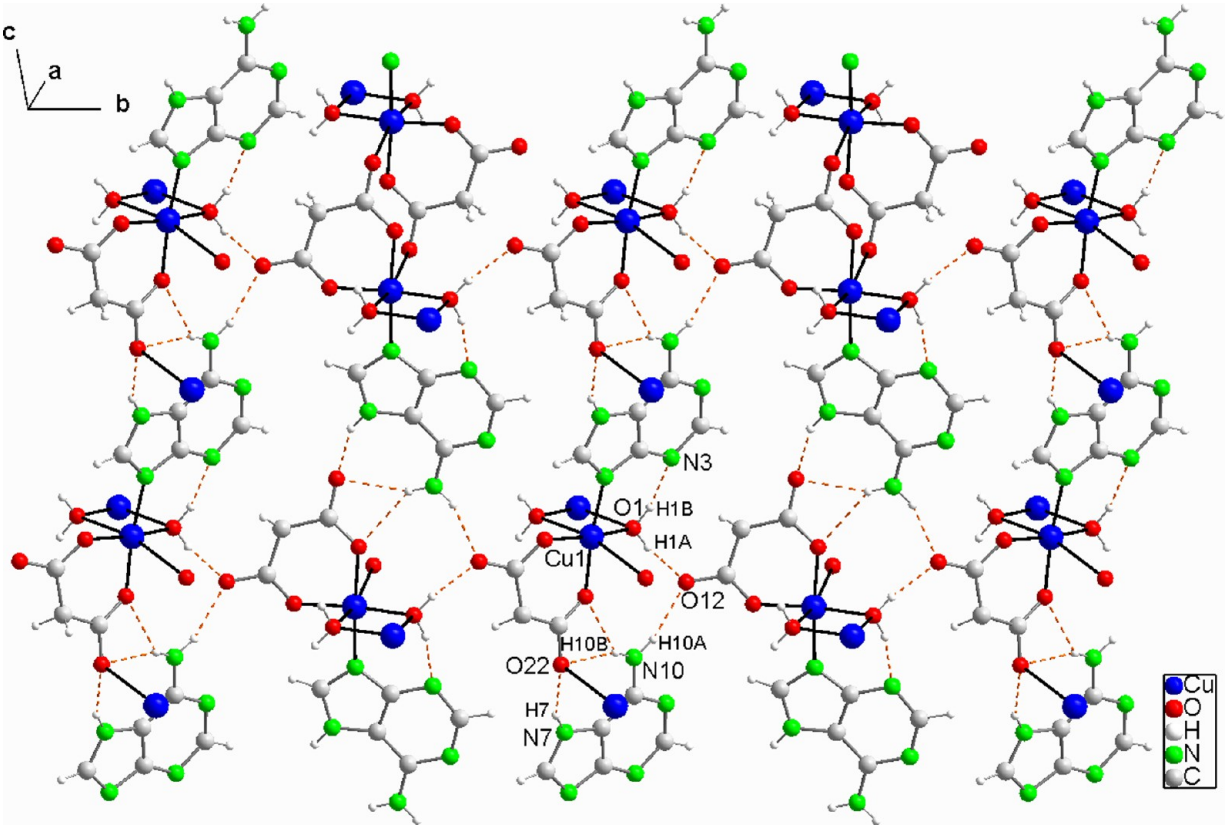


**Figure 6.** View of the supramolecular structure of **2** in the plane *bc*, showing the formation of sheets. Hydrogen bonds are shown as orange dashed lines.

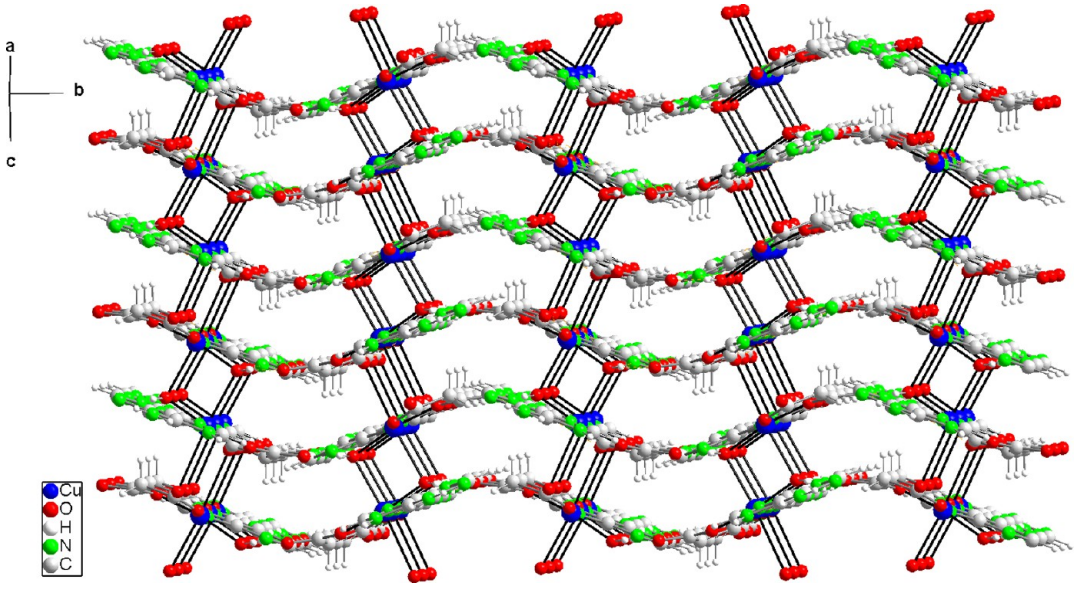


**Figure 7.** View of 3D supramolecular framework of **2** showing the wavy layers along the *b* axis.

SM4 of the Supporting Information) in which the uncoordinated malonate O22 acts as an acceptor and an amino N−H bond of Hade as a donor and N−H···O hydrogen bonds involving the N−H imidazole of Hade and the coordinated malonate O21 to give a ring with graphic set $R_2^2(9)$, as shown in Figure 9. The second amine hydrogen atom and the hydrogen atoms of water molecules form hydrogen bonds with one another and with uncoordinated oxygen atoms or pyrimidine nitrogen atom N1 to give a three-dimensional network (Figure 10). Details of the hydrogen bonding in **3** are given in Table 4.

**Spectroscopic Studies of Complexes.** The infrared spectrum of the uncoordinated malonate anion is characterized by two bands at 1700 $cm^{-1}$ [$\nu_{as}$(COO)] and 1400 $cm^{-1}$ [$\nu_s$(COO)], in addition to medium intensity bands for $\delta$(OCO) at 800 and 700 $cm^{-1}$.[31] The IR spectra of the complexes contain several bands that can be assigned to the malonate ligand. Specifically, in the three complexes the


dx.doi.org/10.1021/cg401455c | *Cryst. Growth Des.* 2014, 14, 249−260

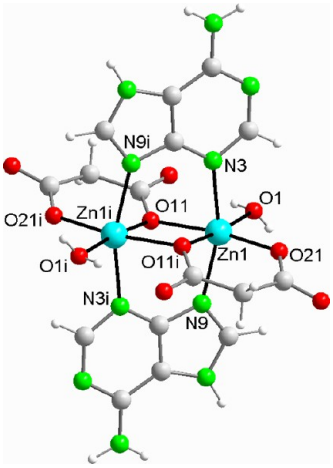


**Figure 8.** Molecular structure of the dimer of **3**. Water molecules of crystallization are omitted for clarity. Symmetry code: (i) $-x, -y, -z + 1$.

$\nu_{as}$(COO) stretching modes appear in the range 1624−1545 $cm^{-1}$, while $\nu_s$(COO) stretching modes appear between 1400 and 1320 $cm^{-1}$. As already seen in the spectra of other malonato complexes, the variability in the number of $\nu_{as}$(COO) bands is explained by the different mode and strength of the metal-carboxylate bond.[32] However, the participation of the carboxylate in different hydrogen bonds may lead to splitting of some bands. In the structural analysis of the complexes reported here, it was observed that malonate ligands exhibit different coordinative behavior, a situation that explains the presence of several bands corresponding to the $\nu_{as}$(COO) stretching modes. For example, in **1**, the malonate acts as a bidentate chelate system and a band is observed at 1584 $cm^{-1}$. In **2**, however, the malonate acts as a tridentate bridging ligand and two bands are observed at 1584 and 1545 $cm^{-1}$. In **3**, the malonate also acts as a tridentate ligand but in this case an oxygen atom coordinates simultaneously to two zinc centers in a bidentate manner to form one asymmetric bridge and three bands at 1624, 1600, and 1564 $cm^{-1}$ are observed. In addition, several absorption bands are observed at higher frequencies (3500−3000 $cm^{-1}$) and these are characteristic of $\nu$(OH) of the hydrogen-bonded water molecules and $\nu(NH_2)$ and $\nu$(NH) of adenine. The shifts in these bands indicate that hydrogen atoms are involved in hydrogen bonding. The bands in the region 1470−1440 $cm^{-1}$, assigned to $\nu$(CN) + $\nu$(CC) modes, indicate coordination of adenine via N9. The weak bands below 600 $cm^{-1}$ are attributed to the $\nu$(MN) and $\nu$(MO) vibrations.

The electronic spectrum of complex **1** in the visible region is dominated by an intense band at around 29100 $cm^{-1}$, which is assigned to an O→Co ligand-to-metal charge-transfer transition. In the range of the d−d transitions, the reflectance spectrum is characteristic of an essentially octahedral symmetry, with two bands around 20900 and 15100 $cm^{-1}$ that can be assigned to $^4T_{1g}\rightarrow{}^4T_{1g}(P)$ and $^4T_{1g}\rightarrow{}^4A_{2g}$ transitions, respectively.[33]

The reflectance spectrum of complex **2** exhibits a strong absorption band near to 30100 $cm^{-1}$, which is assigned to a O→Cu ligand-to-metal charge-transfer transition, whereas the d−d absorptions are observed as a medium-broad band at around 15000 $cm^{-1}$, which is consistent, when considered along with the X-ray structural data described above, with a distorted octahedral structure for this polymeric compound.[33]

**Thermogravimetric Analysis.** Thermogravimetric analysis experiments were conducted to investigate the thermal stability of the crystalline materials. The results are given in (see Figures SM6-SM9 of the Supporting Information). For complex **1**, the first two consecutive weight loss steps occurred in the temperature range of 25−148 °C, and these correspond to the release of lattice water molecules. At higher temperature, the complex started to decompose. A new two-step mass loss process was observed and the third step, between 150−404 °C, corresponds principally to pyrolysis of the malonate ligand and this produced $CO_2$ and $H_2O$. The degradation of the rest of the organic part in the solid residue took place in the fourth step, which occurred in the temperature range of 404−450 °C, with one violent exothermic peak at 426 °C. This process represents the loss of about 39% of the sample and produced $CO_2$, $H_2O$, CO, and nitrogen oxides due to decomposition of the remaining malonate and total decomposition of Hade in an overlapping process. The final residue had 24.11% of the weight of the initial sample and appears to be $Co_2O_3$ (calculated: 24.07%).[34] In the TGA curve of complex **2**, the 3D network is

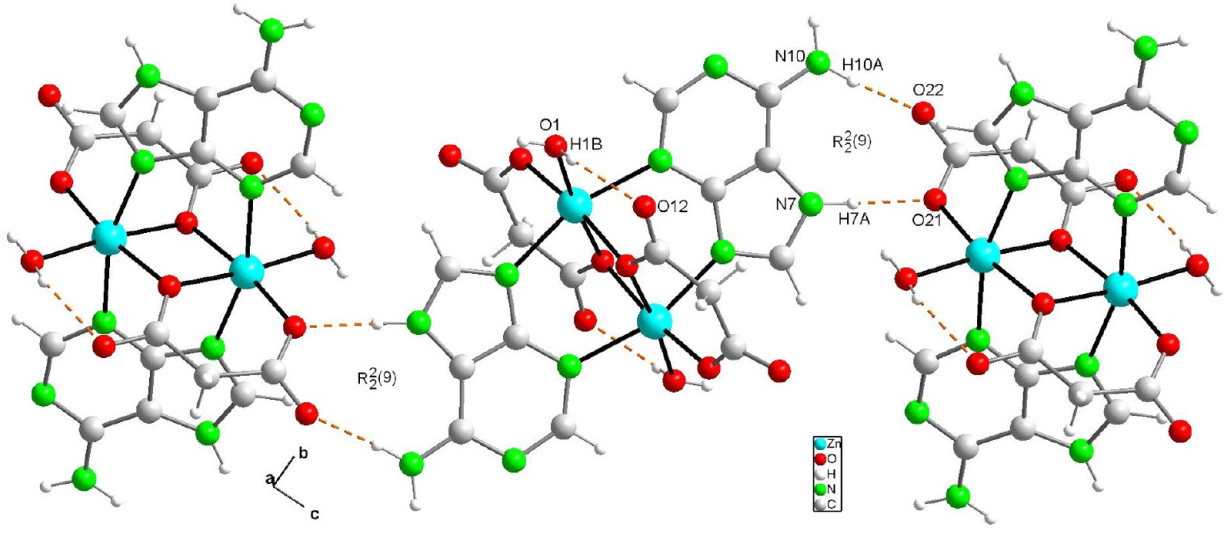


**Figure 9.** Hydrogen bonding linking the dimers in **3**. Hydrogen bonds are shown as orange dashed lines.


dx.doi.org/10.1021/cg401455c | *Cryst. Growth Des.* 2014, 14, 249−260

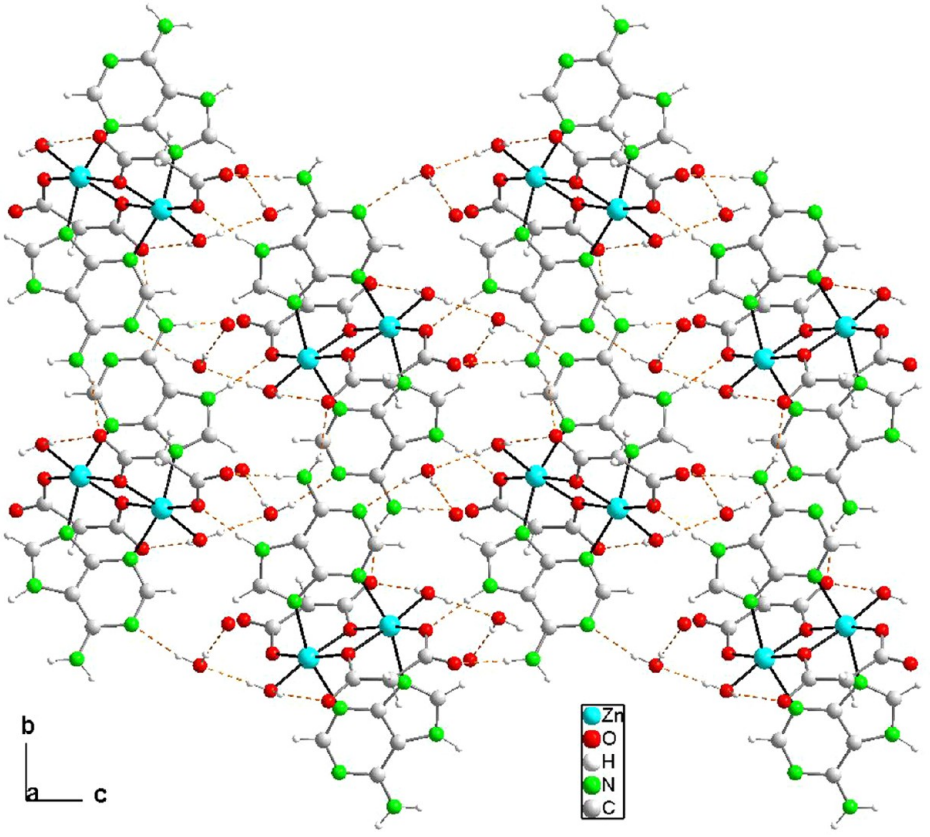


**Figure 10.** View of the 3D supramolecular framework of **3** showing the hydrogen-bonding interactions as orange dashed lines.

stable up to 200 °C, indicating the absence of crystallization water molecules. In this case, decomposition occurred with two consecutive weight loss steps (75.06%) upon further heating. These steps were complete at 435 °C. This weight loss is assigned to consecutive removal of aqua, malonate, and adenine ligands, and it produced $H_2O$, $CO_2$, and traces of CO, $N_2O$, NO, and $NO_2$. The residual solid seemed to be copper(II) oxide (calculated: 26.95%). The thermogravimetric curve for compound **3** shows similar weight loss behavior to compound **1**. The first weight loss is assigned to the removal of crystallization water molecules. Thermal analysis shows a first step between room temperature and 146 °C with a weight loss of around 7%. The next three consecutive weight loss steps occurred in the range of 146−635 °C (74.14%). These correspond to decomposition of the network, starting with removal of ligand aqua molecules and the beginning of malonate ligand pyrolysis to give $H_2O$ and $CO_2$. The process continues with the termination of the malonate ligand pyrolysis and the beginning of adenine ligand decomposition, ending with decomposition of this ligand in the range of 483−635 °C, as revealed by the release of nitrogen oxides and some $H_2O$ and $CO_2$. The residual solid appears to be zinc oxide (calculated: 24.04%).

**Magnetic Properties.** The magnetic behavior of **2** was studied in the range of 2−300 K, and the plot of $\chi_M T$ versus $T$ is shown in Figure 11. At 300 K, $\chi_M T$ is 0.89 emu·mol$^{-1}$·K, which is the value expected for two magnetically quasi-isolated spin doublets ($g$ > 2.00). Upon cooling, the compound from room temperature (300 K) to 50 K, $\chi_M T$ increased slightly. Below 50 K, the $\chi_M T$ value decreased rapidly on further cooling before reaching a minimum of 0.24 emu mol$^{-1}$ K at 2 K. Such magnetic behavior is indicative of antiferromagnetic interactions of copper(II) centers. From the structural point of view, complex **2** is an alternating one-dimensional system in which the copper(II) ions are linked by malonate and aqua bridging ligands. From the magnetic point of view, however, taking into account the relatively long Cu-bridging malonate distance (ca. 2.80 Å), compound **2** may be considered as a binuclear complex in which two copper(II) ions are linked by two aqua ligands, in contrast to the behavior observed in $[Cu_2(\mu\text{-}OH_2)_2(suc)(NN)_2(NO_3)_2]_n$ (suc = succinate, NN = bpy or phen).[35] In addition, for a carboxylate-bridged copper(II) system where the CuOCOCu exchange pathway involves an equatorial position at one copper(II) ion and an axial position of the nearest neighboring copper(II), as in **2**, one would

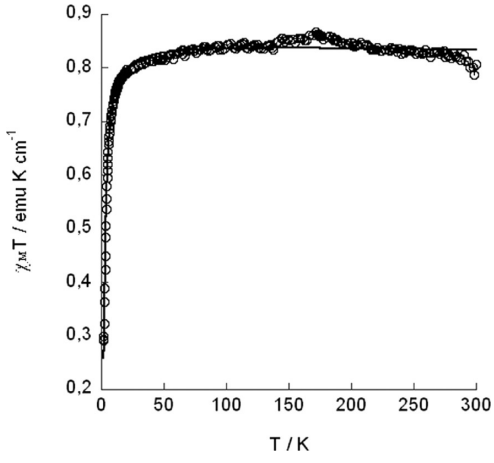


**Figure 11.** Thermal dependence of the $\chi_M T$ product for compound **2**. Solid line is the best fit from eq (1) (see text).


dx.doi.org/10.1021/cg401455c | *Cryst. Growth Des.* 2014, 14, 249−260

expect very weak ferromagnetic behavior.[32] Upon consideration of this situation, and assuming the hypothesis of the molecular field approximation to account for the possible very small interactions through the malonate ligands, the experimental data for the dinuclear Cu(II) entity of **2** were fitted by applying the Bleaney–Bowers formula[36] using the Hamiltonian $H = -JS_1S_2$. The fit was achieved by minimization of $R = \Sigma(\chi_m T_{calc} - \chi_m T_{obs})^2/(\chi_m T_{obs})^2$ by a least-squares procedure. The best-fit parameters obtained are $J = -3$ cm$^{-1}$, and $g = 2.12$ with an $R$ of $3.2 \times 10^{-3}$.

Oxo-bridged Cu(II) binuclear complexes are among the families that have been most widely studied experimentally since they provide examples of the simplest case of magnetic interaction involving only two unpaired electrons. A vast amount of research shows that the nature and strength of the exchange are chiefly affected by the Cu–O–Cu bond angle ($\theta$). The classical correlation between the experimental exchange coupling constants ($2J$) and the Cu–O–Cu bond angles indicates that the complexes are generally antiferromagnetic for $\theta > 98°$ and ferromagnetic for $\theta < 98°$.[37] Moreover, it has been suggested that out-of-plane displacement of the hydrogen atoms of the aqua or hydroxo bridge also has an important influence on exchange.[37c] Small values of $\theta$ appear to be combined with large out-of-plane displacements of the hydrogen atoms, and both of these favor ferromagnetic character, as does decreasing Cu–O distance. In short, the structural requirements for an oxo-bridged Cu(II) binuclear compound to have strong ferromagnetic coupling are that it has small Cu–O–Cu angles, short Cu–O distances, large out-of-plane shifts of the hydrogen atoms on the bridge, and hinge-distorted $Cu_2O_2$. In **2**, the exchange pathway between each pair of $Cu^{II}$ ions runs essentially through two $\mu$-aqua bridges with a Cu–O–Cu angle of 97.03° and out-of-plane shifts of the hydrogen atoms of 53.0° (H1A) and 57.5° (H1B). The observed interactions resulting from these competing influences are antiferromagnetic. This behavior contrasts with that observed in $[Cu_2(\mu_5\text{-btb})(\mu\text{-OH})(\mu\text{-}H_2O)]_n$ ($H_3$btb = benzene-1,2,3-tricarboxylic acid), a 1D coordination polymer with $Cu_2$ units and three magnetically active exchange pathways that link the copper(II) ions through a long $\mu$-aqua bridge, an anti-syn carboxylate bridge, and a mixed $\mu$-hydroxo + syn–syn carboxylate bridge. At temperatures higher than 30 K, this system behaves as isolated $Cu_2$ units with strong ferromagnetic Cu–Cu coupling through the $\mu$-hydroxo and syn–syn carboxylate bridges.[38]

**EPR Spectroscopy.** The X-band EPR spectrum of a polycrystalline sample of compound **2** recorded at room temperature is shown in Figure 12. The spectrum consists of an almost axial signal with $g_{\|} > g_{\perp}$. This spectrum is consistent with a $d_{x^2-y^2}$ ground orbital state, as expected for a 4 + 1 + 1 geometry.[39] The lack of hyperfine patterns, particularly at the $g_2$ peaks, is attributed to narrowing effects[40] due to exchange interactions, a situation in agreement with the bulk magnetic properties of the complex. The spectrum was fitted,[41] assuming the anisotropic $S = 1/2$ spin Hamiltonian $\hat{H} = \beta\hat{\mathbf{S}}\tilde{\mathbf{g}}\mathbf{H}$, resulting in values of 2.270 and 2.132 for the EPR parameters $g_{\|}$ and $g_{\perp}$, respectively.

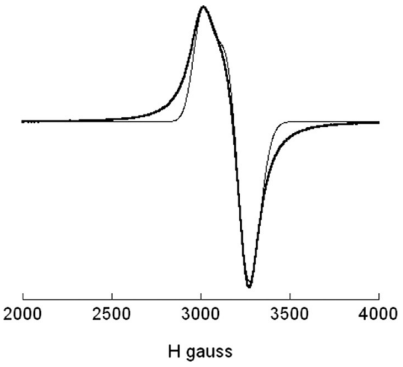


**Figure 12.** X-band EPR spectrum from a polycrystalline sample of **2** at r.t. Solid line: experimental spectrum; fine line: theoretical curve.

## CONCLUSIONS

The structural results show that the combination of malonate and adenine ligands with different centers allows the isolation of three kinds of compounds (i.e., ionic $[Co(7H\text{-ade-}N9)_2(H_2O)_4][Co(\kappa^2\text{-mal})(H_2O)_2]\cdot 4H_2O$ (**1**), coordination polymer $_\infty{}^1[Cu(\mu\text{-mal})(7H\text{-ade-}N9)(\mu_2\text{-}H_2O)]$ (**2**), and dimer $[Zn_2(\mu\text{-mal})_2(\mu\text{-}7H\text{-ade-}N3,N9)_2(H_2O)_2]\cdot 2H_2O$ (**3**). The combination of H-bonds and $\pi$-stacks of adenine on the M(mal) core led to diverse metallo-supramolecular architectures. These observations indicate that the self-assembling ability of adenine and the strong $\pi$-stacking of adenine are effective tools for the control of molecular arrangement. The results described here also demonstrate that the relative orientation of the carboxylate groups in the malonate dianion is a crucial factor in determining both the molecular and the metallo-supramolecular structure of the products from the reactions with adenine and $Co^{II}$, $Cu^{II}$, and $Zn^{II}$ salts.

In the coordination polymer $_\infty{}^1[Cu(\mu\text{-mal})(7H\text{-ade-}N9)(\mu_2\text{-}H_2O)]$ (**2**), the $Cu^{II}$ ion, which is chelated, remains in the same plane as the carboxylato groups of malonate, whereas the unidentate coordinated copper(II) deviates considerably from this plane and the oxygen atom becomes axial. As a consequence of the coupling of orbitals of different symmetry, the magnetic interactions are expected to be weak ferromagnetic and the final antiferromagnetic behavior is due to the copper(II) ions linked by aqua bridging ligands alternating in the one-dimensional system with copper(II) ions linked by malonate bridges.

## ASSOCIATED CONTENT

### Supporting Information

Additional structural information is provided in Figures SM1 to SM5 (CCDC 695244, 605247, and 605249). Relevant spectroscopic properties, thermal stability information, and magnetic properties can be found in Figures SM6–SM9 and SM10, respectively. CIF files are available. This material is available free of charge via the Internet at http://pubs.acs.org.

## AUTHOR INFORMATION

### Corresponding Author

*E-mail: alfonso.castineiras@usc.es. Tel: +34 88181 4951. Fax: +34 88181 5090.

### Notes

The authors declare no competing financial interest.

## ACKNOWLEDGMENTS

Financial support from Research Groups FQM-283 and FQM-174 (Junta de Andalucía) and MICINN-Spain (Project MAT2010-15594) is acknowledged.

## REFERENCES


(1) (a) Desiraju, G. R. *Angew. Chem., Int. Ed. Engl.* **1995**, *34*, 2311. (b) Hollingsworth, M. D. *Science* **2002**, *295*, 2410. (c) Trask, A. V.; Motherwell, W. D. S.; Jones, W. *Cryst. Growth Des.* **2005**, *5*, 1013. (d) Desiraju, G. R. *Angew. Chem., Int. Ed.* **2007**, *46*, 8342.

(2) Davis, A. V.; Yeh, R. M.; Raymond, K. N. *Proc. Natl. Acad. Sci. U.S.A.* **2002**, *99*, 4793.

(3) Biradha, K.; Fujita, M. In *Crystal Design, Structure and Function (Perspectives in Supramolecular Chemistry)*; Desiraju, G. R., Ed.; Wiley: Chichester, West Sussex, England, 2003; Vol. 7.

(4) (a) Li, L.-L.; Lin, K.-J.; Ho, C.-J.; Sun, C.-P.; Yang, H.-D. *Chem. Commun.* **2006**, 1286. (b) Desiraju, G. R. *J. Am. Chem. Soc.* **2013**, *135*, 9952. (c) Beobiden, G.; Castillo, O.; Cepeda, J.; Luque, A.; Pérez-Yáñez, S.; Román, P.; Thomas-Gipson, J. *Coord. Chem. Rev.* **2013**, *257*, 2716.

(5) Steed, J. W.; Atwood, J. L. *Supramolecular Chemistry*; John Wiley & Sons: New York, 2000.

(6) *Crystal Engineering: The Design and Application of Functional Solids*; Seddon, K. R.; Zaworotko, M. J., Eds.; NATO, ASI series; Kluwer: Dordrecht, The Netherlands, 1998.

(7) (a) Desiraju, G. R. *J. Chem. Soc., Chem. Commun.* **1991**, 426. (b) Infantes, L.; Motherwell, S. *CrystEngComm* **2002**, *4*, 454.

(8) Desiraju, G. R. *J. Chem. Sci.* **2010**, *122*, 667.

(9) Yang, E.-C.; Zhao, H.-K.; Feng, Y.; Zhao, X.-J. *Inorg. Chem.* **2009**, *48*, 3511 and references cited therein.

(10) Kurmoo, M. *Chem. Soc. Rev.* **2009**, *38*, 1353 and references cited therein.

(11) (a) Rodríguez-Martín, Y.; Hernández-Molina, M.; Delgado, F. S.; Pasán, J.; Ruíz-Pérez, C.; Sanchíz, J.; Lloret, F.; Julve, M. *CrystEngComm* **2002**, *4*, 522. (b) Pérez-Yañez, S.; Castillo, O.; Cepeda, J.; García-Terán, J. P.; Luque, A.; Román, P. *Eur. J. Inorg. Chem.* **2009**, 3889. (c) Caballero, A. B.; Rodríguez-Diegues, A.; Lezama, L.; Salas, J. M. *Cryst. Growth Des.* **2012**, *12*, 3583.

(12) Castiñeiras, A.; García-Santos, I.; González-Pérez, J. M.; Niclós-Gutiérrez, J. Proceedings of the 9th European Biological Inorganic Chemistry Conference, Wroclaw, Poland, Sept 2-6, 2008; Kozlowski, H., Ed.; Medimond: Pianoro, Italy, 2008; 135.

(13) *Bruker APEX2 Software*, V2.0-1; Bruker AXS Inc.: Madison, Wisconsin, 2005.

(14) Sheldrick, G. M. *SADABS. Program for Empirical Absorption Correction of Area Detector Data*. University of Göttingen: Germany, 1997.

(15) Sheldrick, G. M. *Acta Crystallogr.* **2008**, *A64*, 112.

(16) Spek, A. L. *J. Appl. Crystallogr.* **2003**, *36*, 7.

(17) Brandenburg, K.; Putz, H. *Diamond, version 3.2*; Crystal Impact GbR: Bonn, Germany, 2009.

(18) Zhao, X.-J.; Zhang, Z.-H.; Wang, Y.; Du, M. *Inorg. Chim. Acta* **2007**, *360*, 1921.

(19) (a) Blackburn, A. V.; Gallucci, J. C.; Gerkin, R. E. *Acta Crystallogr.* **1990**, *B46*, 712. (b) *Acta Crystallogr.* **1991**, *C47*, 282.

(20) (a) de Meester, P.; Skapski, A. C. *J. Chem. Soc., Dalton Trans.* **1973**, 1596. (b) Atria, A. M.; Garland, M. T.; Baggio, R. *Acta Crystallogr.* **2012**, *C67*, m275.

(21) (a) Etter, M. C. *Acc. Chem. Res.* **1990**, *23*, 120. (b) Etter, M. C.; MacDonald, J. C.; Bernstein, J. *Acta Crystallogr.* **1990**, *B46*, 256. (c) Etter, M. C. *J. Phys. Chem.* **1991**, *95*, 4601. (d) Bernstein, J.; Davis, R. E.; Shimoni, L.; Chang, N.-L. *Angew. Chem., Int. Ed.* **1995**, *34*, 1555.

(22) (a) Mackaren, J. K.; Sanchiz, J.; Gili, P.; Janiak, Ch. *New J. Chem.* **2012**, *36*, 1596. (b) Maclaren, J. K.; Janiak, Ch. *Inorg. Chim. Acta* **2012**, *389*, 183. (c) Ward, M. D. *Struct. Bonding (Berlin, Ger.)* **2009**, *132*, 1. (d) Gilli, G.; Gilli, P. The Nature of the Hydrogen Bond. In *Outline of a Comprehensive Hydrogen Bond Theory*; Oxford University Press: Oxford, 2009.

(23) Janiak, Ch. *J. Chem. Soc., Dalton Trans.* **2000**, 3885.

(24) (a) García-Terán, J. P.; Castillo, O.; Luque, A.; García-Couceiro, U.; Román, P.; Lloret, F. *Inorg. Chem.* **2004**, *43*, 5761. (b) Aoki, K.; Salam, M. A.; Munakata, Ch.; Fujisawa, I. *Inorg. Chim. Acta* **2007**, *360*, 3658. (c) Choquesillo-Lazarte, D.; Brandi-Blanco, M. P.; García-Santos, I.; González-Pérez, J. M.; Castiñeiras, A.; Niclós-Gutiérrez, J. *Coord. Chem. Rev.* **2008**, *252*, 1241. (d) Patel, D. K.; Domínguez-Martín, A.; Brandi-Blanco, M. P.; Choquesillo-Lazarte, D.; Nurchi, V. M.; Niclós-Gutiérrez, J. *Coord. Chem. Rev.* **2012**, *256*, 193.

(25) Melník, M.; Kabešová, M.; Koman, M.; Macášková, Ľ; Holloway, C. E. *J. Coord. Chem.* **2000**, *90*, 177.

(26) Hendrickson, J. B. *J. Am. Chem. Soc.* **1967**, *89*, 7036.

(27) *Structure Correlations*, v. 2; Bürgi, H.-B.; Dunitz, J. D., Eds.; VCH: Weinheim, Germany, 1994.

(28) (a) Yang, E. C.; Chan, Y.-N.; Ziu, H.; Wang, Z.-Ch; Zhao, X.-J. *Cryst. Growth Des.* **2009**, *9*, 4933. (b) An, J.; Geib, S. J.; Rosi, N. L. *J. Am. Chem. Soc.* **2009**, *131*, 8376. (c) An, J.; Farha, O. K.; Hupp, J. T.; Pohl, E.; Yeh, J. I.; Rosi, N. L. *Nat. Commun.* **2012**, *3*, 604.

(29) (a) Mastropietro, T. F.; Armentano, D.; Marino, N.; De Munno, G. *Polyhedron* **2007**, *26*, 4945. (b) Stylianov, K. C.; Warren, J. E.; Chong, S. Y.; Rabone, J.; Bacsa, J.; Bradshaw, D.; Rosseinsky, M. J. *Chem. Commun.* **2011**, *47*, 3389.

(30) Wei, C. H.; Jacobson, K. B. *Inorg. Chem.* **1981**, *20*, 356.

(31) Nakamoto, K. *Infrared and Raman Spectra of Inorganic and Coordination Compounds*, 15th ed.; John Wiley & Sons: New York, 1997.

(32) Sanchíz, J.; Rodríguez-Martín, Y.; Ruíz-Pérez, C.; Mederos, A.; Lloret, F.; Julve, M. *New J. Chem.* **2002**, *26*, 1624.

(33) Lever, A. B. P. *Inorganic Electronic Spectroscopy*, 2nd ed; Elsevier: Amsterdam, 1984.

(34) Bermejo, E.; Carballo, R.; Castiñeiras, A.; Lago, A. B. *Coord. Chem. Rev.* **2013**, *257*, 2639.

(35) Ghoshal, D.; Maji, T. K.; Mostafa, G.; Sain, S.; Lu, T.-H.; Ribas, J.; Zangrande, E.; Chaudhuri, N. R. *Dalton* **2004**, 1687.

(36) Bleaney, B.; Bowers, K. *Proc. R. Soc. London, Ser. A* **1952**, *214*, 451.

(37) (a) Crawford, V. H.; Richardson, H. W.; Wasson, J. R.; Hodgson, D. J.; Hadtfield, W. E. *Inorg. Chem.* **1976**, *15*, 2107. (b) Khan, O. *Molecular Magnetism*; VCH publishers: New York, 1993. (c) Ruiz, E.; Alemany, P.; Alvarez, S.; Cano, J. *J. Am. Chem. Soc.* **1997**, *119*, 1297.

(38) Habib, H. A.; Sanchiz, J.; Janiak, Ch. *Dalton Trans.* **2008**, 4877.

(39) Hathaway, J.; Billing, D. E. *Coord. Chem. Rev.* **1970**, *5*, 143.

(40) Anderson, P. W. *J. Phys. Soc. Jpn.* **1954**, *9*, 316.

(41) *Win EPR-Simfonia 1.25*, Bruker Analytik GmgH: Karlsruhe, FRG, 1994−1996.